

**Reply to Comment on
“Reevaluation of the parton distribution of strange quarks in the nucleon”**

E.C. Aschenauer,¹ H.E. Jackson,² S. Joosten,³ K. Rith,⁴ G. Schnell,^{5,6} and C. Van Hulse⁵

(On behalf of the HERMES Collaboration)

¹*Brookhaven National Laboratory, Upton, New York 11772-5000, USA*

²*Physics Division, Argonne National Laboratory, Argonne, Illinois 60439-4843, USA*

³*Department of Physics, University of Illinois, Urbana, Illinois 61801-3080, USA*

⁴*Physikalisches Institut, Universität Erlangen-Nürnberg, 91058 Erlangen, Germany*

⁵*Department of Theoretical Physics, University of the Basque Country UPV/EHU, 48080 Bilbao, Spain*

⁶*IKERBASQUE, Basque Foundation for Science, 48013 Bilbao, Spain*

(Dated: December 2, 2015 – version 2.0)

A Comment on the recently published reevaluation of the polarization-averaged parton distribution of strange quarks in the nucleon using final data on the multiplicities of charged kaons in semi-inclusive deep-inelastic scattering (DIS) is reviewed. Important features of the comparison of one-dimensional projections of the multidimensional HERMES data are pointed out. A test of the leading-order extraction of $x_B S(x_B)$ using the difference between charged-kaon multiplicities is repeated. The results are consistent with leading-order predictions within the uncertainties in the input data, and do not invalidate the earlier extraction of $x_B S(x_B)$.

I. INTRODUCTION

In the *Comment on “Reevaluation of the parton distribution of strange quarks in the nucleon”*, the Author presents a number of studies to conjecture that the analysis presented in Ref. [1] likely suffers from effects that invalidate the leading-order analysis used in that publication. For the studies presented part of the charged-hadron multiplicity database of Ref. [2] was used.

In our opinion, the Author has drawn erroneous conclusions, using HERMES data on pion multiplicities [2], regarding the extraction of the strange-quark parton distribution $x_B S(x_B)$ from charged-kaon multiplicities. In addition, his check of this extraction using the properties of the charged-kaon difference multiplicity and its derivative, the K' “multiplicity” [cf. Eq. (4)], is invalidated by the large uncertainties in the values used for relevant fragmentation functions (FFs) and parton distributions. We present below the results from a repetition of that analysis using a range of parton distribution sets. The spread in those results precludes credible conclusions and demonstrates the sensitivity of the analysis to poorly known input data (unfavored FFs, strange-quark distributions, and mixed singlet and nonsinglet quantities).

Before going into detail we would like to recall some of the motivations for the analysis presented in Ref. [1]:

- the strangeness distribution is a poorly known quantity: due to its usual suppression in most observables it is difficult to access;
- charge- and flavor-separated FFs are, at this point, still not well constrained. Indeed, the FFs for kaons differ significantly in the various phenomenological extractions, employing strong assumptions to reduce the number of independent functions. One of the reasons for this is the dominance of e^+e^- annihilation data in those extractions that does not easily allow for a charge separation of the FFs. For the analysis of the strange-quark distribution in Ref. [1] an isoscalar extraction was employed to avoid as much as possible this complication of involving badly constrained FFs, e.g., only charge-summed FFs are needed from the global analysis of kaon FFs, an aspect that validates the use of the FF phenomenology, which is dominated by e^+e^- annihilation data;
- we reiterate here again the statement in Ref. [1] that “while a full next-to-leading order (NLO) extraction would be preferred, such a procedure using semi-inclusive DIS data is not currently available,” and that as such “a leading-order extraction is an important first step”.

II. DATA ANALYSES AND COMPARISONS

The Author of the Comment [3] offers a number of checks that in his opinion should/could support or disprove the conclusions drawn in Ref. [1]. In Sec. III B the charged-pion sum is analyzed, which has little to do with the analysis presented in [1]. As the Author points out himself, because of u -quark dominance in pion fragmentation, the component of the charged-pion multiplicity generated by strange-quark fragmentation should be small, e.g., only a few %. Consequently, given currently attainable measurement precision, charged-pion multiplicities provide no information on properties of strange quarks. It follows that the body of discussion in Sec. III concerning features of the leading-order (LO) description of the pion multiplicity sum is not directly relevant to the extraction of $x_B S(x_B)$ from kaon data reported by HERMES.

One salient point is the observation of “the almost identical shapes of the pion and kaon distributions.” Our comparison of the shapes is presented in Fig. 1 where the kaon values have been renormalized to the pion values in the region of $0.1 < x_B < 0.45$ where both curves flatten, presumably due to the absence of a contribution from strange-quark fragmentation. While similar, the shapes are not nearly identical. While the similarity is an interesting observation, it may be coincidental, and likely can only be disentangled in a full QCD analysis, which is at this point still out of reach. Until then possible implications on the LO extraction of $x_B S(x_B)$ presented in Ref. [1] cannot be assessed.

For all the discussion, a grave conceptual misunderstanding must be pointed out, also because it appears to cloud the analyses [4] referred to by the Author to strengthen his case. Although not related to the kaon multiplicities analyzed in Ref. [1], the Author indulges in *invalid comparisons* of pion multiplicity values (last paragraph of Sec. III A). Different one-dimensional projections of a multiparameter observable, such as a multiplicity, are not topologically equivalent. In the case discussed in the Comment [3], the corresponding sections in the x_B and Q^2 projections of the observable span different, albeit, overlapping regions of the Born space accepted in the measurement. From setting the values of the observables drawn from these two different sections equal [e.g., erroneously assuming that the average multiplicity should correspond to the multiplicity at (event-weighted) average kinematics], the unjustified conclusion is drawn that the measurements presented in Ref. [2] are not consistent. In contrast to the Author’s claim that “a

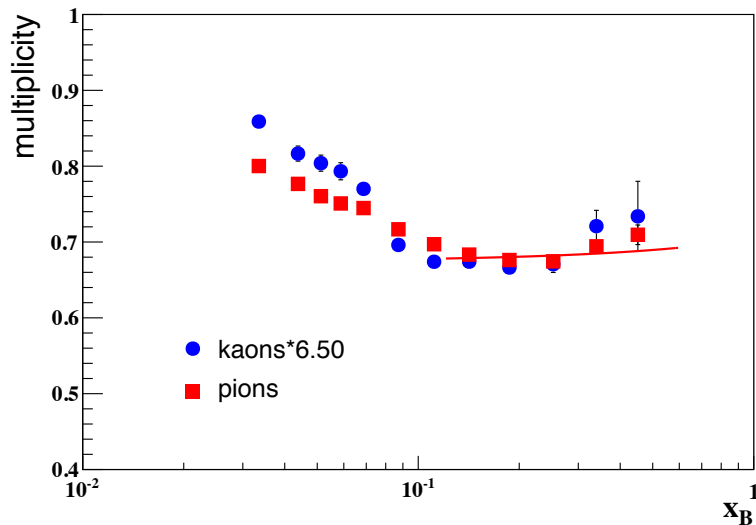


FIG. 1. Comparison of the shapes of multiplicities corrected to 4π of charged kaons and pions in semi-inclusive DIS from a deuterium target, as a function of Bjorken x_B . The kaon multiplicities are scaled to agree with those of pions in the range of x_B where both distributions flatten. Data are plotted at the average x_B of each individual x_B bin.

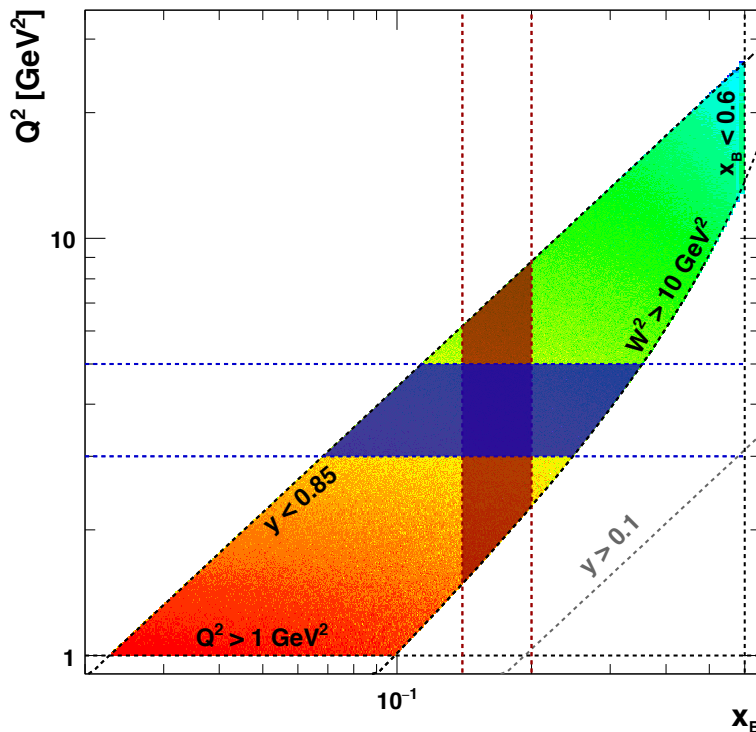


FIG. 2. Born space in (x_B, Q^2) corresponding to the multiplicities reported in Ref. [2]. Kinematic regions covered by two data points with similar average kinematics, as discussed in the Comment [3], are superimposed (highlighted slices in either x_B or Q^2). Note that the color coding is logarithmic, and that most of the events [$\mathcal{O}(70\%)$] in either of the two bins are in fact not shared.

large part of the data [in the two representations] are the same”, Fig. 2 clearly demonstrates the contrary: only a small part of the kinematic regions covered by those two data points do overlap.

As an example, multiplicities in the x_B - z representation involve integrations over Q^2 (as well as $P_{h\perp}$). Consequently, when comparing to theoretical predictions, the same integration has to be performed, e.g., for the LO parton-model

expression one has to evaluate

$$\mathcal{M}^\pi(x_B, z) = \frac{\sum_q e_q^2 \int_{Q_{\min}^2(x_B)}^{Q_{\max}^2(x_B)} q(x_B, Q^2) D_q^\pi(z, Q^2) dQ^2}{\sum_q e_q^2 \int_{Q_{\min}^2(x_B)}^{Q_{\max}^2(x_B)} q(x_B, Q^2) dQ^2}, \quad (1)$$

or an analogous integration for any other type.

The Author points out that the (very) low- x_B region can be neglected in the discussion of the two bins in question ($3 \text{ GeV}^2 < Q^2 < 5 \text{ GeV}^2$ of the z - Q^2 representation, and $0.14 < x_B < 0.2$ of the z - x_B representation in Ref. [2]), as the relevant Q^2 bin is large enough not to include the low- x_B data. Indeed, x_B is larger than about 0.07. But already from Fig. 1 of the Comment [3] it should have been clear that the average x_B in that bin sits basically at the minimum of the multiplicity distribution, such that the multiplicity averaged over that x_B range ($0.07 \lesssim x_B \lesssim 0.35$) must be larger than the multiplicity at that average x_B , as it is indeed found.

This clarification of how to use the multiplicity database [2] is an important enough aspect for *any* analysis of these multiplicities, especially when attempting to compare to theory predictions, such that it deserves to be again highlighted here.

In Sec. IV, the Author turns from the isoscalar extraction to an analysis involving the difference between K^+ and K^- multiplicities, e.g.,

$$\frac{dN^{K^{\text{diff}}}}{dN^{\text{DIS}}} \equiv \frac{d(N^{K^+} - N^{K^-})}{dN^{\text{DIS}}} \quad (2)$$

$$\stackrel{\text{LO}, s=\bar{s}}{=} \frac{(u_v + d_v)(4D_u^{K^+} - 4D_{\bar{u}}^{K^+} + D_d^{K^+} - D_{\bar{d}}^{K^+})}{5Q + 2S}, \quad (3)$$

where the second line is obtained at LO assuming $s(x_B) = \bar{s}(x_B)$, and where $Q \equiv u + \bar{u} + d + \bar{d}$ and $S \equiv s + \bar{s}$ are as defined in Ref. [1], $D_q^{K^+}$ are the quark-flavor separated FFs¹ into K^+ , and u_v (d_v) the up (down) valence distributions.

First of all, it should be noted that the difference multiplicity is inherently nonsinglet and consequently sensitive to the flavor structure of the fragmentation process. Also, the features of the Q^2 evolution of this quantity is different than that of the sum multiplicity. This applies even more to the so-called K' “multiplicity”, a mixture of the nonsinglet difference and the isoscalar charge-sum multiplicity (dN^K/dN^{DIS}):

$$\frac{dN^{K'}}{dN^{\text{DIS}}} \equiv \frac{5Q + 2S}{Q} \frac{dN^K}{dN^{\text{DIS}}} - \frac{5Q + 2S}{u_v + d_v} \frac{dN^{K^{\text{diff}}}}{dN^{\text{DIS}}} \quad (4)$$

$$\stackrel{\text{LO}, s=\bar{s}}{=} 8D_u^{K^+} + 2D_{\bar{d}}^{K^+} + \frac{S}{Q} D_S^K \quad (5)$$

$$= 8D_u^{K^-} + 2D_{\bar{d}}^{K^-} + \frac{S}{Q} D_S^K. \quad (6)$$

In the Comment [3] an extraction of the kaon charge-difference multiplicity (and of the K' “multiplicity”) is carried out using MSTW08 [5] and alternatively NNPDF3.0 [6] LO parton-distribution functions (PDFs) as well as a determination of the relevant nonstrange fragmentation functions “from the data at high x_B , exactly as was done by HERMES for D_Q^K ”. The Author states that contrary to expectation the observable decreases at low x_B , and that “it is hard to expect that the Q^2 dependence of $D_{\bar{u}}^{K^+} + D_{\bar{d}}^{K^+}$ can fully explain the shape.” This is concluded to be “an indication of the failure of the conventional LO pQCD parton model approach.”

We have repeated such analysis using a set of LO PDFs, namely NNPDF3.0 and MSTW08 (as in the Comment [3]) as well as CTEQ6 [7] and NNPDF2.3 [8]. These were then used to evaluate the K' multiplicities according to Eq. (4). In addition, we have followed the Author’s suggestion of using the “high- x_B limit” of $dN^{K'}/dN^{\text{DIS}}$ to normalize the unfavored fragmentation combination ($8D_{\bar{u}}^{K^+} + 2D_{\bar{d}}^{K^+}$), and used the data base of Ref. [9] (DSS) to generate the Q^2 dependence of those.² (The “high- x_B limit” was obtained by evaluating in the last x_B bin a polynomial fit to the NNPDF3.0 data points for $x_B > 0.1$.) Alternatively, the original DSS FFs [9] were used.³ Together with $Sf dz D_S^K$

¹ It is implicitly assumed in this text that FFs are integrated over the relevant range in the fractional hadron energy $0.2 < z < 0.8$.

² Here we deviate from the path of the Author by not using QCDNUM for performing the Q^2 evolution.

³ It should be noted that the DSS analysis is based, in part, on a preliminary unpublished version of the HERMES data on charged-meson multiplicities from a hydrogen target.

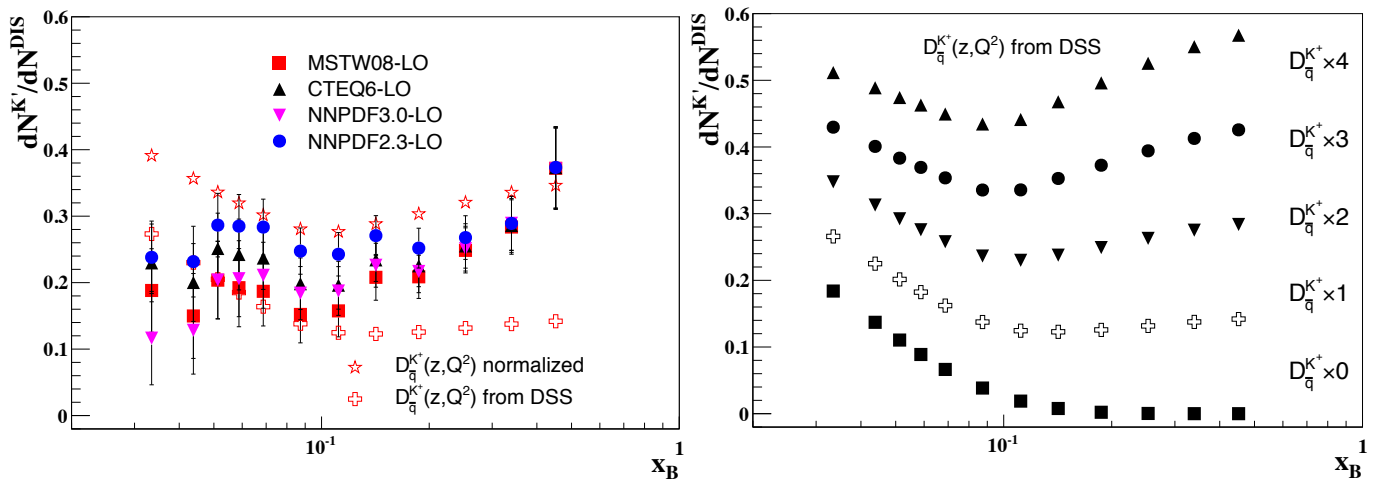


FIG. 3. Left: K' “multiplicities” corrected to 4π of charged kaons in semi-inclusive DIS from a deuterium target, as a function of x_B , evaluated with Eq. (4) using MSTW08 (squares), CTEQ6 (upward triangles), NNPDF3.0 (downward triangles), and NNPDF2.3 (full circles) LO PDF sets. Also shown are the LO predictions [e.g., Eq. (5)] using DSS FFs (crosses) or using the high- x_B HERMES data to constrain the unfavored \bar{u} and \bar{d} to K^+ FFs (stars). For both the crosses and stars, $S \int dz dZ_S^K$ from Ref. [1] and Q from NNPDF3.0 were used. Note that uncertainties on PDFs or FFs—when available at all—were not propagated, but only total experimental uncertainties. Right: Equation (5) evaluated in the same way as the crosses to the left, but for a range of scaled DSS unfavored nonstrange kaon FFs [using scaling factors from 0 (bottom) to 4 (top) as in Fig. 2 (left) in the Comment]. As in the Comment [3], all points were evaluated at the average Q^2 of each individual x_B bin.

from Ref. [1] and Q from NNPDF3.0 these two sets of FFs were used to evaluate Eq. (5). For the Q^2 evolution of the PDFs the package LHAPDF [10] was used. Our results are presented in Fig. 3.

In contrast to the results in the Comment [3], one can find a reasonable agreement between the HERMES extraction of $dN^{K'}/dN^{DIS}$ and the latter leading-order prediction, when uncertainties in the FFs and PDFs are accounted for. The following observations are worthwhile mentioning:

- first it should be noted that the DSS predictions for the kaon FFs, particularly for the unfavored FFs are, to say the least, uncertain. In the DSS compilation all the kaon unfavored FFs are assumed to be equal, and in particular $D_{\bar{u}}^{K^+} = D_{\bar{d}}^{K^+}$. Taking into account uncertainties in the DSS compilation of the unfavored nonstrange kaon FFs [11], a broad range of “LO predictions” based on Eq. 5 is obtained filling essentially the range between the squares and circles in the right of Fig. 3;
- the two choices for the unfavored nonstrange K^+ FFs, namely DSS (crosses in Fig. 3 left) and the ones derived from the “high- x_B limit”, e.g., the last x_B bin (stars in Fig. 3 left), envelop the region populated by the HERMES data folded with various LO PDF sets;
- as expected, the results for the extracted values of $dN^{K'}/dN^{DIS}$ converge to a common locus for $x_B > 0.1$, since for negligible sea-quark contributions (common among the chosen PDF sets) Eq. (4) reduces simply to ten times the K^- multiplicity⁴, independent of the values for the valence distributions. In the region $x_B < 0.1$ the spread in the extracted values of $dN^{K'}/dN^{DIS}$ becomes large reflecting the large variation in the sea-quark PDFs over the four sets used. While NNPDF2.3 results in a reasonable description when compared to the set of unfavored nonstrange FFs derived from the “high- x_B limit,” the overall choices of PDF and FF sets result in a wide range of “predictions” for either side of Eq. (7) of the Comment [3], i.e., Eqs. (4) and (5) herein. This clearly demonstrates the large sensitivity of these nonsinglet quantities to subtleties in the choice of PDFs and FFs;
- using the Q^2 evolution of the DSS FF set, we cannot reproduce the shapes of the curves in the Comment’s Fig. 2 (left) [3]. We present the quantity of Eq. (5) on the right of Fig. 3. There is a strong underlying Q^2 dependence that leads to the rise of the K' “multiplicity” with x_B for large values of the unfavored FFs, something not visible in the version of this figure in the Comment [3]. The strong Q^2 dependence of the unfavored DSS kaon FFs is depicted also in Fig. 4;

⁴ It is interesting to note that the DSS prediction in this region significantly undershoots the data pointing to underestimated strength in the unfavored nonstrange kaon FFs.

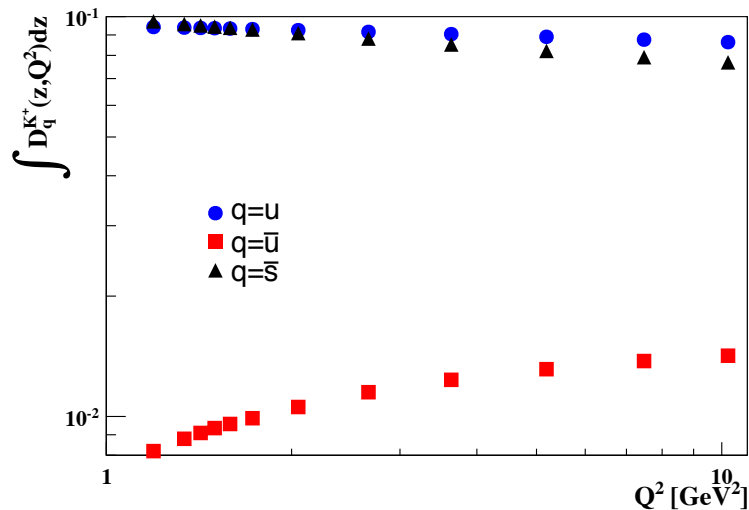


FIG. 4. The Q^2 dependence of the DSS favored u and \bar{s} (scaled by a factor $1/7$) as well as the unfavored \bar{u} to K^+ fragmentation functions. Note that for the DSS FF set $D_{\bar{u}}^{K^+} = D_{\bar{d}}^{K^+}$. Chosen Q^2 values correspond to the average Q^2 of the x_B bins in Figs. 3 and 5.

- even more striking than the lack of the high- x_B rise for the considerably increased DSS FFs is the behavior of the lowest curve in the corresponding figure of the Comment [3]: when the unfavored FFs are set to zero, the x_B behavior is driven entirely by the last term in Eq. (5). SD_S^K rapidly reaches zero above $x_B = 0.1$ [1]. As Q remains sizable in that range of x_B also the ratio $\frac{S}{Q}D_S^K$ should approach zero (as it does on the right of Fig. 3 for the corresponding squares). In Fig. 2 left of the Comment [3], however, instead of going to zero that curve rises with x_B above $x_B = 0.1$. We have no explanation for this apparent discrepancy;
- the rapidly rising values as x_B increases make extracting a “high- x_B limit,” as recommended in the Comment [3], very tenuous at best. Unlike the situation with the original isoscalar extraction of $S(x_B)$ [1], where a high- x_B limit was used to constrain a favored combination of FFs and where the multiplicity levels out and thus has a meaningful limit, it appears that the notion of a “high- x_B limit” is not applicable in this case, where both the last term in Eq. (5) and the unfavored FFs in that equation are suppressed quantities.

The large spread in the PDF-dependent extractions of $dN^{K'}/dN^{\text{DIS}}$ as well as the spread between the predictions for this quantity using the values of the unfavored FFs from DSS and those from a nominal “high- x_B limit” argue against using this quantity as a benchmark for testing the validity of the LO formalism.

We have also extracted the quantity [cf. Eq. (3)]

$$\frac{5Q + 2S}{4(u_v + d_v)} \frac{dN^{K^{\text{diff}}}}{dN^{\text{DIS}}} \stackrel{\text{LO}, s=\bar{s}}{=} 4 \left(D_u^{K^+} - D_{\bar{u}}^{K^+} \right) + \left(D_d^{K^+} - D_{\bar{d}}^{K^+} \right) \quad (7)$$

that is shown in the right panel of Fig. 2 of the Comment [3] with the same assumptions used in the extraction above. Four sets of LO PDFs were used again in the calculation of the quantity. The result is presented in Fig. 5 together with two LO predictions in terms of sums of FFs. In contrast to the result shown in the Comment [3] the agreement of the measurement with the LO predictions is reasonable except at the low x_B values, and in view of the crudeness of the data we have for kaon FFs, perhaps as good as we can expect at this time. Most striking is the spread originating from the use of the various PDF sets. This poses a serious concern about the sensitivity of this quantity to available PDF sets. The corresponding plot in the Comment [3] thus appears to be an exaggeration of the disagreement between LO prediction and data.

III. CONCLUSION

In contrast to the kaon multiplicities, those of the pions cannot be satisfactorily described in LO. Until this problem is understood, it is difficult to relate features of the pion data to the behavior of the kaon data. Our studies involving charged-kaon difference multiplicities do not corroborate the results presented in the Comment [3]. Rather we find,

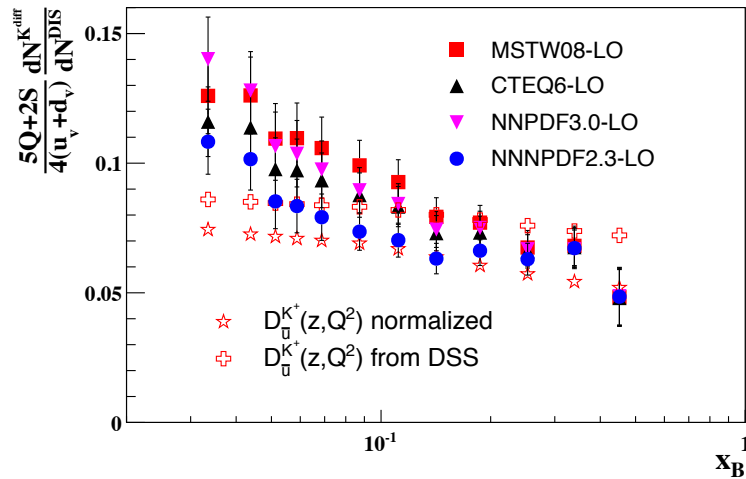


FIG. 5. The scaled charge-difference multiplicities $\frac{dN^{K^{\text{diff}}}}{dN^{\text{DIS}}} \cdot \frac{5Q+2S}{4(u_v+d_v)}$ of charged kaons in semi-inclusive DIS from a deuterium target, as a function of x_B , evaluated using various LO PDF sets [MSTW08 (squares), CTEQ6 (upward triangles), NNPDF3.0 (downward triangles), and NNPDF2.3 (circles)], compared with the LO predictions based on solely DSS FFs (crosses) and DSS FFs combined with unfavored kaon FFs constrained using HERMES data at high x_B (stars). As in the Comment [3], all points were evaluated at the average Q^2 of each individual x_B bin.

within the uncertainties dictated by the current limited knowledge of strange FFs and even LO PDF sets, that the difference data is consistent with LO predictions.

We reiterate again the statement from Ref. [1] that while a NLO extraction of $S(x_B)$ would be preferred, such a procedure using SIDIS data is not currently feasible, and a LO extraction is an important first step.

ACKNOWLEDGMENTS

This work was supported by the German Bundesministerium für Bildung und Forschung (BMBF), and the Deutsche Forschungsgemeinschaft (DFG); the Basque Foundation for Science (IKERBASQUE) and the UPV/EHU under program UFI 11/55; as well as the U.S. Department of Energy (DOE) and the National Science Foundation (NSF).

IV. APPENDIX: TABLES OF MULTIPLICITIES USED

Tables I–III, and IV list the multiplicity values used herein including the average values of x_B and Q^2 for π^+ , π^- , K^+ , and K^- , respectively. The total uncertainties on the multiplicities, obtained by adding in quadrature both statistical and systematic uncertainties, are propagated for all quantities computed, in particular, the multiplicity differences and sums.

-
- [1] A. Airapetian *et al.* (HERMES Collaboration), *Phys. Rev.* **D89**, 097101 (2014), arXiv:1312.7028 [hep-ex].
[2] A. Airapetian *et al.* (HERMES Collaboration), *Phys. Rev.* **D87**, 074029 (2013), arXiv:1212.5407 [hep-ex].
[3] M. Stolarski, *Phys. Rev.* **D92**, 098101 (2015), arXiv:1407.3721 [hep-ex].
[4] E. Leader, A. V. Sidorov, and D. B. Stamenov, (2015), arXiv:1506.06381 [hep-ph].
[5] A. D. Martin, W. J. Stirling, R. S. Thorne, and G. Watt, *Eur. Phys. J.* **C63**, 189 (2009), arXiv:0901.0002 [hep-ph].
[6] R. D. Ball *et al.* (NNPDF), *JHEP* **04**, 040 (2015), arXiv:1410.8849 [hep-ph].
[7] J. Pumplin, D. R. Stump, J. Huston, H. L. Lai, P. M. Nadolsky, and W. K. Tung, *JHEP* **07**, 012 (2002), hep-ph/0201195.
[8] J. Rojo (NNPDF Collaboration), (private communications).
[9] D. de Florian, R. Sassot, and M. Stratmann, *Phys. Rev.* **D75**, 114010 (2007), hep-ph/0703242.
[10] A. Buckley, J. Ferrando, S. Lloyd, K. Nordström, B. Page, M. Rüfenacht, M. Schönherr, and G. Watt, *Eur. Phys. J.* **C75**, 132 (2015), arXiv:1412.7420 [hep-ph].
[11] M. Epele, R. Llubaroff, R. Sassot, and M. Stratmann, *Phys. Rev.* **D86**, 074028 (2012), arXiv:1209.3240 [hep-ph].

TABLE I. Multiplicities corrected to 4π of π^+ mesons in semi-inclusive DIS from a deuterium target, as a function of Bjorken x_B .

$\langle x_B \rangle$	$\langle Q^2 \rangle$ [GeV ²]	Multiplicity	Statistical uncertainty	Systematic uncertainty
0.033	1.19	0.422	0.002	0.010
0.044	1.34	0.420	0.003	0.010
0.051	1.42	0.408	0.003	0.008
0.059	1.50	0.405	0.003	0.008
0.069	1.59	0.406	0.002	0.007
0.087	1.73	0.394	0.001	0.005
0.112	2.05	0.382	0.002	0.006
0.142	2.67	0.378	0.002	0.005
0.187	3.63	0.378	0.002	0.004
0.253	5.19	0.379	0.003	0.005
0.340	7.48	0.389	0.005	0.005
0.451	10.23	0.393	0.010	0.005

TABLE II. Multiplicities corrected to 4π of π^- mesons in semi-inclusive DIS from a deuterium target, as a function of Bjorken x_B .

$\langle x_B \rangle$	$\langle Q^2 \rangle$ [GeV ²]	Multiplicity	Statistical uncertainty	Systematic uncertainty
0.033	1.19	0.378	0.002	0.008
0.044	1.34	0.357	0.002	0.007
0.051	1.42	0.353	0.003	0.006
0.059	1.50	0.346	0.003	0.006
0.069	1.59	0.339	0.002	0.006
0.087	1.73	0.323	0.001	0.005
0.112	2.05	0.315	0.002	0.004
0.142	2.67	0.306	0.002	0.004
0.187	3.63	0.298	0.002	0.003
0.253	5.19	0.296	0.002	0.003
0.340	7.48	0.305	0.004	0.004
0.451	10.23	0.316	0.009	0.004

TABLE III. Multiplicities corrected to 4π of K^+ mesons in semi-inclusive DIS from a deuterium target, as a function of Bjorken x_B .

$\langle x_B \rangle$	$\langle Q^2 \rangle$ [GeV ²]	Multiplicity	Statistical uncertainty	Systematic uncertainty
0.033	1.19	0.084	0.001	0.004
0.044	1.34	0.083	0.001	0.004
0.051	1.42	0.080	0.001	0.004
0.059	1.50	0.080	0.001	0.004
0.069	1.59	0.079	0.001	0.004
0.087	1.73	0.073	0.001	0.003
0.112	2.05	0.073	0.001	0.003
0.142	2.67	0.072	0.001	0.003
0.187	3.63	0.074	0.001	0.003
0.253	5.19	0.074	0.001	0.004
0.340	7.48	0.080	0.003	0.004
0.451	10.23	0.075	0.006	0.004

TABLE IV. Multiplicities corrected to 4π of K^- mesons in semi-inclusive DIS from a deuterium target, as a function of Bjorken x_B .

$\langle x_B \rangle$	$\langle Q^2 \rangle$ [GeV ²]	Multiplicity	Statistical uncertainty	Systematic uncertainty
0.033	1.19	0.048	0.001	0.002
0.044	1.34	0.043	0.001	0.002
0.051	1.42	0.044	0.001	0.002
0.059	1.50	0.042	0.001	0.002
0.069	1.59	0.040	0.001	0.002
0.087	1.73	0.034	0.000	0.002
0.112	2.05	0.031	0.001	0.002
0.142	2.67	0.032	0.001	0.002
0.187	3.63	0.029	0.001	0.001
0.253	5.19	0.029	0.001	0.002
0.340	7.48	0.031	0.002	0.002
0.452	10.24	0.038	0.004	0.002